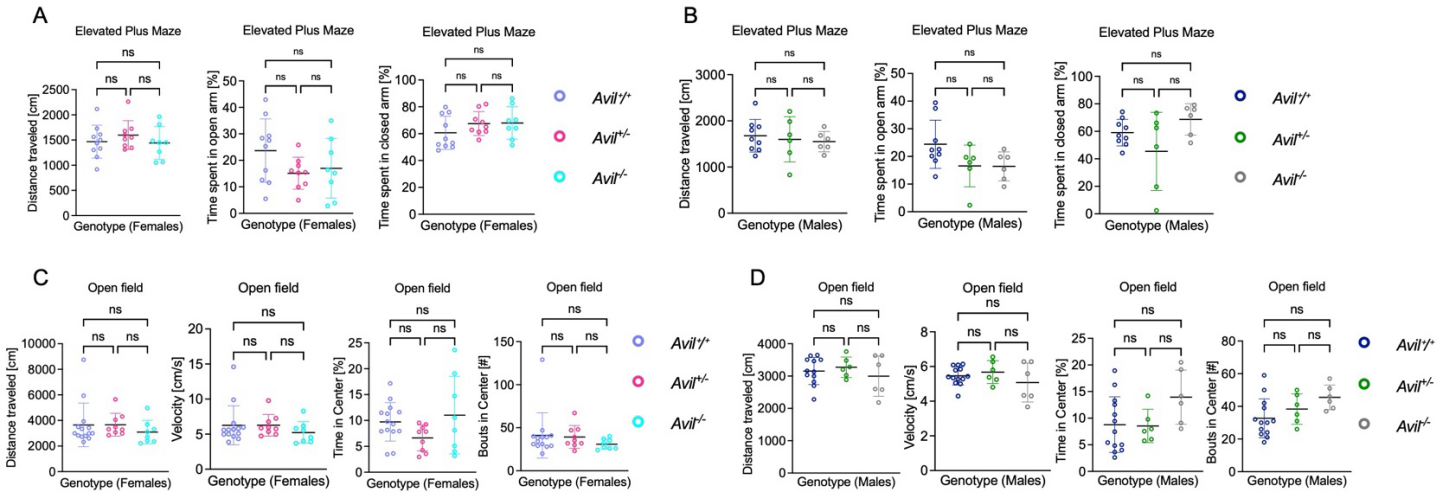
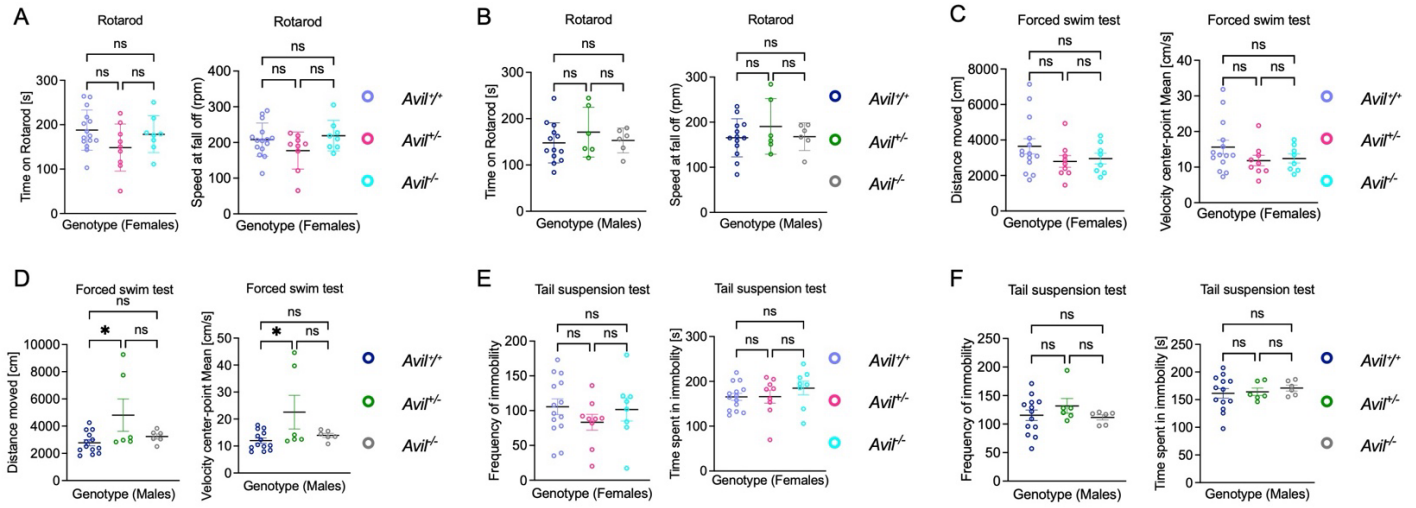
A
Avil+/+
Avil fl/+;Cre
Avil fl/fl;Cre
Brain
Lung
Skeletal Muscle
Pancreas
Stomach
Small intestine
Large intestine
B
Avil+/+
Avil+/-
Avil-/-
Brain
Pancreas
Spleen
Kidney
Lung
Liver
Heart
Stomach
Small intestine
Large intestine
Paw

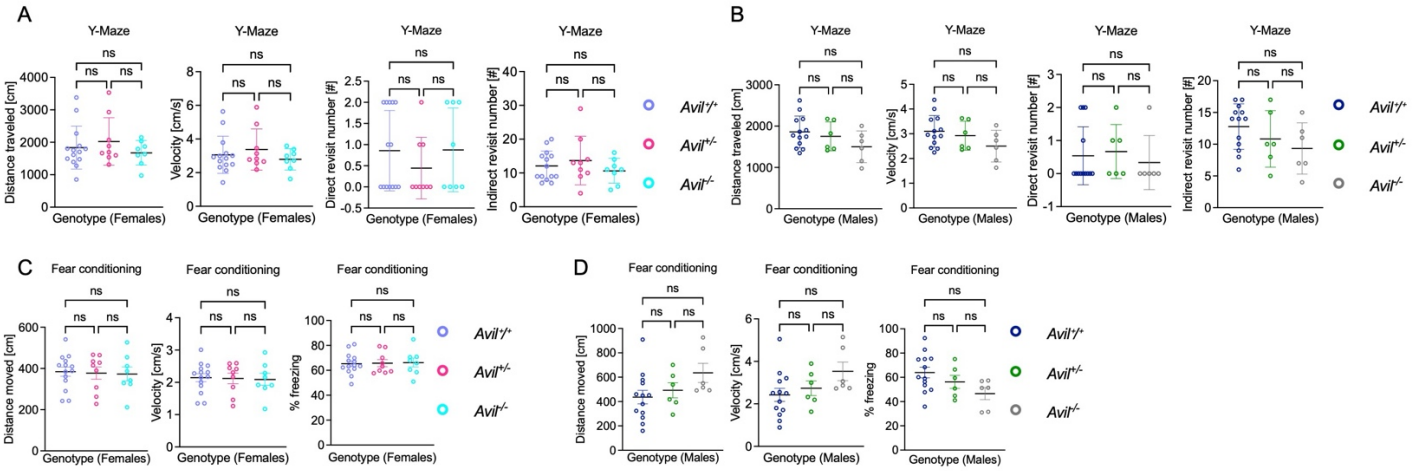
Supplemental Figure 1. Systemic *Avil* deletion is well tolerated without major histological abnormalities. Representative images of hematoxylin and eosin (H&E) staining in tissue from 4-month-old $Avil^{+/+}$, $Avil^{fl/+;Cre}$, and $Avil^{fl/fl;Cre}$ conditional KO mice **(A)** and $Avil^{+/+}$, $Avil^{+/-}$, and $Avil^{-/-}$ constitutive KO mice **(B)**. Scale bars indicate 200 µm.



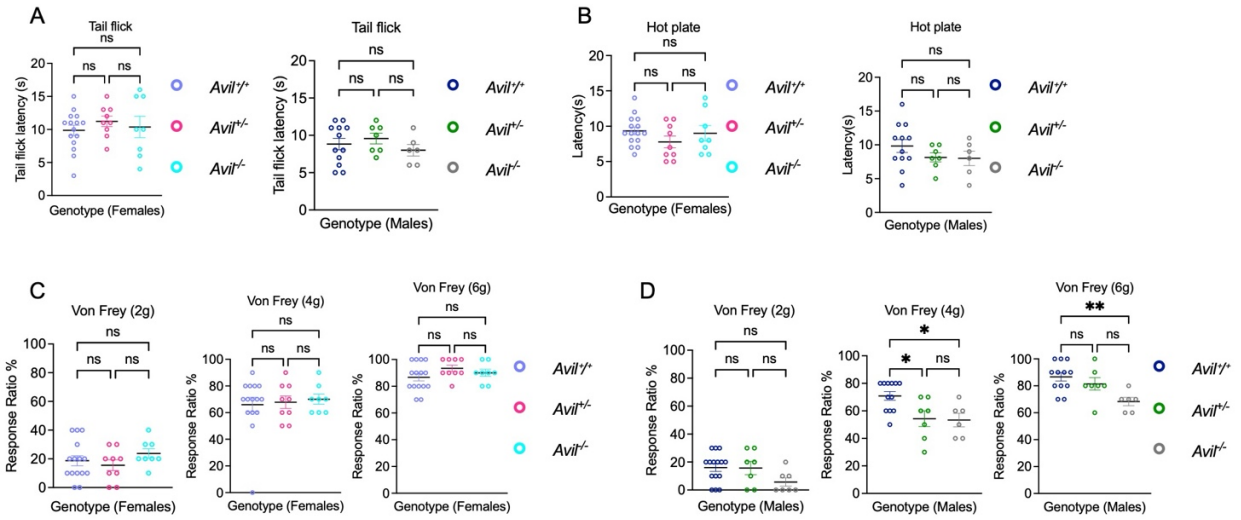
Supplemental Figure 2. *Avil* KO mice display normal anxiety-like behavior and exploratory activity. (A and **B)** Anxiety-like behavior in the elevated plus maze (EPM). Total distance traveled (cm) and time spent in closed and open arms as a percent (%) of total time for female **(A)** and male **(B)** $Avil^{+/+}$ (female, n=10; male, n=9), $Avil^{+/-}$ (female, n=9; male, n=6), $Avil^{-/-}$ (female, n=8; male, n=6) mice in the elevated plus maze. **(C** and **D)** General locomotion, exploratory, and anxiety-like behavior in the open field test. Total distance traveled (cm), average velocity (cm/s), time in center field as a percent (%) of total time, and total bouts in center field (#) of female **(C)**, male **(D)** $Avil^{+/+}$ (female, n=14; male, n=12), $Avil^{+/-}$ (female, n=9; male, n=6), $Avil^{-/-}$ (female, n=8; male, n=6) mice during the open field test. Each data point represents an individual mouse. Error bars represent mean ± S.D. Statistical significance was calculated by one-way ANOVA with Tukey's post-hoc multiple-comparisons test (all graphs in panels A, B, and D and the third graph in panel C) or, for non-normally distributed data, by the non-parametric Kruskal-Wallis test with Dunn's multiple-comparisons test (the first, second, and fourth graphs in panel C). Graph positions are counted from left to right within each panel. ns $P > 0.05$.



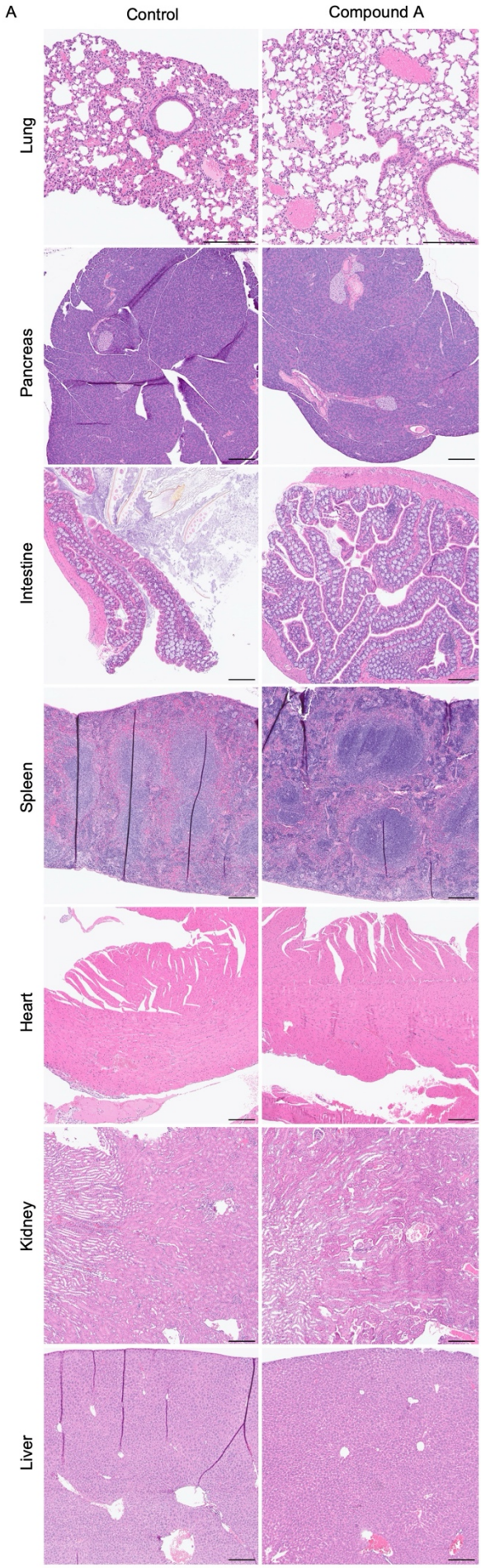
Supplemental Figure 3. *Avil* KO mice display normal motor coordination and depression-like behavior. (A and **B)** Motor coordination on the rotarod. Average latency to fall off the rotating rod (s) and average speed at fall off (rpm) for female **(A)** and male **(B)** *Avil*$^{+/+}$ (female, n=15; male, n=13), *Avil*$^{+/-}$ (female, n=9; male, n=6), *Avil*$^{-/-}$ (female, n=8; male, n=6) mice during the rotarod test. **(C–F)** Baseline depression-like behavioral comparisons between *Avil*$^{-/-}$ and littermate controls. **(C** and **D)** Distance traveled (cm) and velocity (cm/s) of female **(C)** and male **(D)** *Avil*$^{+/+}$ (female, n=14; male, n=13), *Avil*$^{+/-}$ (female, n=9; male, n=6), *Avil*$^{-/-}$ (female, n=8; male, n=6) mice during the forced swim test. **(E** and **F)** Time spent immobile (s) and frequency of immobility in female **(E)** and male **(F)** *Avil*$^{+/+}$ (female, n=14; male, n=13), *Avil*$^{+/-}$ (female, n=9; male, n=6), *Avil*$^{-/-}$ (female, n=8; male, n=6) mice during the tail suspension test. Each data point represents the average of six replicates per individual mouse **(A** and **B)** or a single mouse **(C–F)**. Error bars represent mean ± S.D. Statistical significance was calculated by one-way ANOVA with Tukey's post-hoc multiple-comparisons test (all graphs in panels A–F). ns $P > 0.05$, $*P \leq 0.05$.



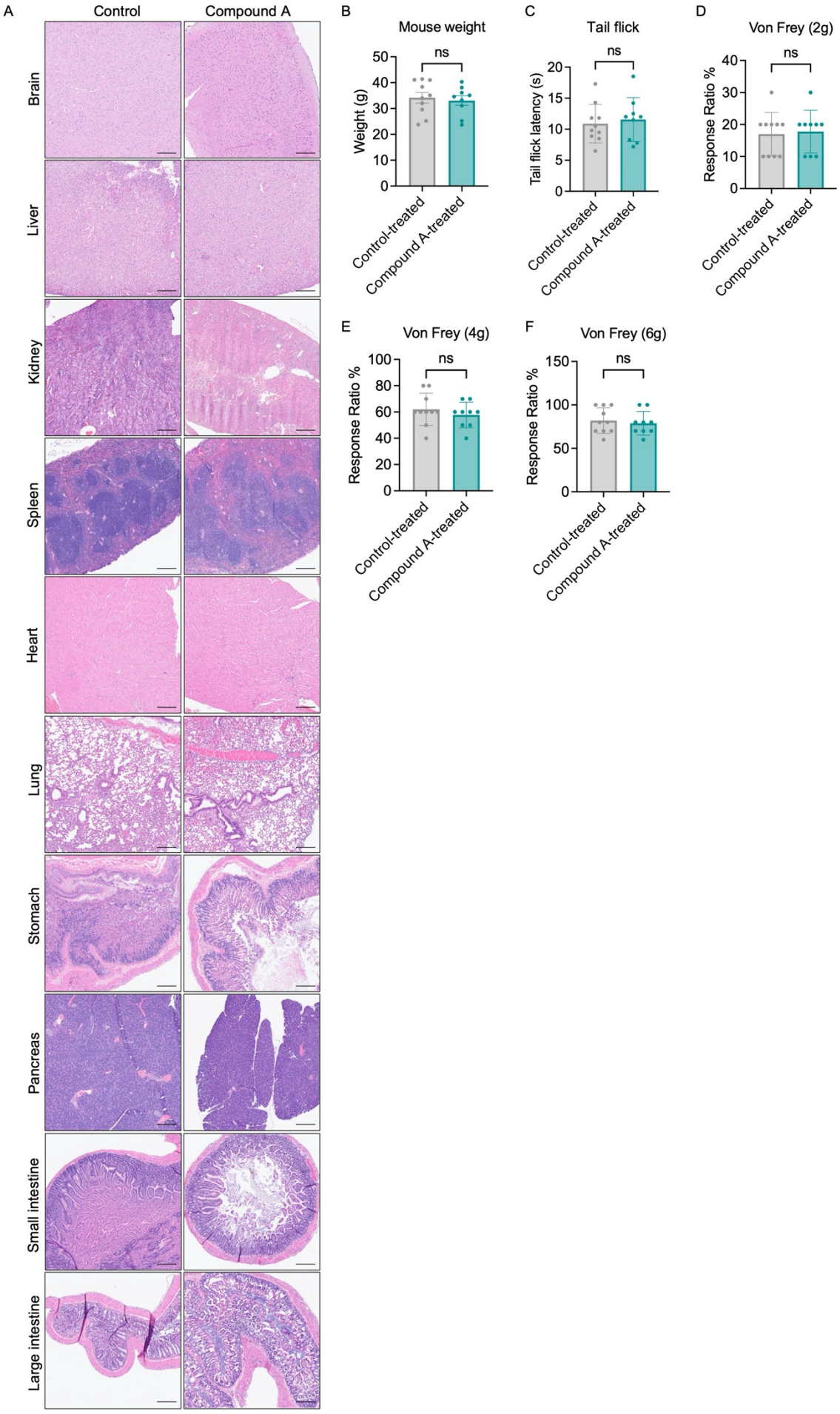
Supplemental Figure 4. Spatial working memory and associative learning are preserved in *Avil* KO mice. Baseline memory behavioral comparisons between *Avil*$^{-/-}$ and littermate controls. **(A** and **B)** Spatial working memory in Y maze. Total distance traveled (cm), velocity (cm/s), number of direct revisits (#), and number of indirect revisits (#) of female **(A)** and male **(B)** *Avil*$^{+/+}$ (female, n=14; male, n=13), *Avil*$^{+/-}$ (female, n=9; male, n=6), *Avil*$^{-/-}$ (female, n=8; male, n=6) mice during the Y-maze test. **(C** and **D)** Associative memory formation in the fear conditioning test. Total distance traveled (cm), average velocity (cm/s), and percentage of time spent immobile (% freezing) for female **(C)** and male **(D)** *Avil*$^{+/+}$ (female, n=16; male, n=13), *Avil*$^{+/-}$ (female, n=9; male, n=6), *Avil*$^{-/-}$ (female, n=6; male, n=6) mice assessed during the context test. Each point represents an individual mouse. Error bars represent mean ± S.D. Statistical significance was calculated by one-way ANOVA with Tukey's post-hoc multiple-comparisons test (the fourth graph in panel A, and all graphs in panels B–D) or, for non-normally distributed data, by the non-parametric Kruskal-Wallis test with Dunn's multiple-comparisons test (the first, second and third graphs in panel A). Graph positions are counted from left to right within each panel. ns P> 0.05.



Supplemental Figure 5. Systemic *Avil* loss preserves nociceptive and tactile sensory functions. (A) Latency to tail flick (s) after exposure to a 48°C water bath in female and male *Avil*$^{+/+}$ (female, n=15; male, n=12), *Avil*$^{+/-}$ (female, n=9; male, n=7), *Avil*$^{-/-}$ (female, n=8; male, n=6) mice. **(B)** Latency to paw lifting (s) after exposure to a 54°C hotplate for female and male *Avil*$^{+/+}$ (female, n=15; male, n=12), *Avil*$^{+/-}$ (female, n=9; male, n=7), *Avil*$^{-/-}$ (female, n=8; male, n=6) mice. Each point represents an individual mouse. **(C** and **D)** Mechanical response rates (%) to increasing filament forces (2-g, 4-g, 6-g) in female **(C)** and male **(D)** *Avil*$^{+/+}$ (female, n=15; male, n=15), *Avil*$^{+/-}$ (female, n=9; male, n=7), *Avil*$^{-/-}$ (female, n=8; male, n=7) mice. Each data point represents an average of ten replicates per individual mouse. Error bars represent mean ± S.D. Statistical significance calculated by one-way ANOVA with Tukey's post-hoc multiple-comparisons test (all graphs in panels A–D). ns $P > 0.05$, *$P \leq 0.05$, **$P \leq 0.01$.


A
Control
Compound A
Lung
Pancreas
Intestine
Spleen
Heart
Kidney
Liver

Supplemental Figure 6. Pharmacologic Avil inhibition is well tolerated without major histological abnormalities. (A) Representative images of H&E staining in tissues from *Avil*$^{+/+}$ mice treated with vehicle (control) or advillin-targeting Compound A (200 mg/kg) for seven days. Scale bars indicate 200 μm.


A
Control
Compound A
Brain
Liver
Kidney
Spleen
Heart
Lung
Stomach
Pancreas
Small intestine
Large intestine
B
Mouse weight
Weight (g)
ns
Control-treated
Compound A-treated
C
Tail flick
Tail flick latency (s)
ns
Control-treated
Compound A-treated
D
Von Frey (2g)
Response Ratio %
ns
Control-treated
Compound A-treated
E
Von Frey (4g)
Response Ratio %
ns
Control-treated
Compound A-treated
F
Von Frey (6g)
Response Ratio %
ns
Control-treated
Compound A-treated

Supplemental Figure 7. Long-term pharmacologic Avil inhibition is well tolerated without sensory or histological abnormalities. (A) Representative images of H&E staining in tissues from *Avil*$^{+/+}$ mice treated with vehicle (control; n=10) or advillin-targeting Compound A (50 mg/kg; n=9) for three weeks. Scale bars indicate 200 μm. **(B)** Weight (g) of control or Compound A (50 mg/kg) treated *Avil*$^{+/+}$ mice. **(C)** Thermal nociception assessed by tail flick latency (s) in control or Compound A (50 mg/kg) treated *Avil*$^{+/+}$ mice. **(D–F)** Mechanical sensitivity was assessed using the Von Frey assay with 2-g **(D)**, 4-g **(E)**, and 6-g **(F)** filaments in control or Compound A (50 mg/kg) treated *Avil*$^{+/+}$ mice. Data are presented as mean ± SD. Statistical analysis was performed using Welch's t-test (B–F). ns $P > 0.05$.